

Comparison of PSS, SVC and STATCOM Controllers for Damping Power System Oscillations

N. Mithulananthan, *Student Member, IEEE*, Claudio A. Cañizares, *Senior Member, IEEE*, John Reeve, *Fellow, IEEE*, and Graham J. Rogers, *Fellow, IEEE*

Abstract— This paper discusses and compares different control techniques for damping undesirable inter-area oscillation in power systems by means of Power System Stabilizers (PSS), Static Var Compensators (SVC) and Shunt Static Synchronous Compensators (STATCOM). The oscillation problem is analyzed from the point of view of Hopf bifurcations, an “extended” eigen analysis to study different controllers, their locations, and the use of various control signals for the effective damping of these oscillations. The comparisons are based on the results obtained for the IEEE 50-machine, 145-bus test system, which is a benchmark for stability analysis.

Index Terms— Power system oscillations, Hopf bifurcations, PSS, SVC, STATCOM.

I. INTRODUCTION

ELECTROMECHANICAL oscillations have been observed in many power systems worldwide [1], [2], [3], [4]. The oscillations may be local to a single generator or generator plant (local oscillations), or they may involve a number of generators widely separated geographically (inter-area oscillations). Local oscillations often occur when a fast exciter is used on the generator, and to stabilize these oscillations, Power System Stabilizers (PSS) were developed. Inter-area oscillations may appear as the systems loading is increased across the weak transmission links in the system which characterize these oscillations [4]. If not controlled, these oscillations may lead to total or partial power interruption [2], [5].

Electromechanical oscillations are generally studied by modal analysis of a linearized system model [2], [6]. However, given the characteristics of this problem, alternative analysis techniques can be developed by using bifurcation theory to effectively identify and control the state variables associated with the oscillatory problem [7], [8], [9], [10]. Among various types of bifurcations, saddle-node, limit-induced, and Hopf bifurcations have been identified as pertinent to instability in power systems [11]. In saddle-node bifurcations, a singularity of a system Jacobian and/or state matrix results in the disappearance

of steady state solutions, whereas, in the case of certain limit-induced bifurcations, the lack of steady state solutions may be associated with system controls reaching limits (e.g. generator reactive power limits); these bifurcations typically induce voltage collapse. On the other hand, Hopf bifurcations describe the onset of an oscillatory problem associated with stable or unstable limit cycles in non linear systems (e.g. interconnected power system).

The availability of Flexible AC Transmission System (FACTS) controllers [12], such as Static Var Compensators (SVC), Thyristor Control Series Compensators (TCSC), Static Synchronous Compensators (STATCOM), and Unified Power Flow Controller (UPFC), has led their use to damp inter-area oscillations [13], [14], [15]. Hence, this paper first discusses the use of bifurcation theory for the study of electromechanical oscillation problems, and then compares the application of PSS, SVC, and STATCOM controllers, proposing a new controller placement technique and a methodology to choose the best additional control signals to damp the oscillations.

The paper is organized as follows: Section II introduces power system modeling and analysis concepts used throughout this paper; thus, the basic theory behind Hopf bifurcations and the modeling and controls of the PSS, SVC and STATCOM controllers used are briefly discussed. Oscillation control using SVC and STATCOM controllers, including a new placement technique, is discussed in Section III. In Section IV, simulation results for the IEEE 50-machine test system are presented and discussed, together with a brief description of the analytical tools used. Finally, the major contributions of this paper are summarized in Section V.

II. BASIC BACKGROUND

A. Power System Modeling

In general, power systems are modeled by a set of differential and algebraic equations (DAE), i.e.

$$\begin{aligned} \dot{x} &= f(x, y, \lambda, p) \\ 0 &= g(x, y, \lambda, p) \end{aligned} \quad (1)$$

where $x \in \mathbb{R}^n$ is a vector of state variables associated with the dynamic states of generators, loads, and other system controllers; $y \in \mathbb{R}^m$ is a vector of algebraic variables associated with steady-state variables resulting from neglecting fast dynamics (e.g. most load voltage phasor magnitudes and angles);

Accepted to *IEEE Trans. Power Systems*, October 2002.

The research work presented here was developed under the financial support of NSERC, Canada, and the E&CE Department at the University of Waterloo.

N. Mithulananthan, C. A. Cañizares, and J. Reeve are with the Department of Electrical & Computer Engineering, University of Waterloo, Waterloo, ON, Canada, N2L-3G1, c.canizares@ece.uwaterloo.ca.

G. Rogers is with Cherry Tree Scientific Software, RR#5 Colborne, Ontario, Canada, K0K-1S0.

$\lambda \in \mathfrak{R}^l$ is a set of uncontrollable parameters, such as variations in active and reactive power of loads; and $p \in \mathfrak{R}^k$ is a set of controllable parameters such as tap and AVR settings, or controller reference voltages.

Bifurcation analysis is based on eigenvalue analyses [16] (small perturbation stability or modal analysis in power systems [6]), as system parameters λ and/or p change in (1) [11]. Hence, linearization of these equations is needed at an equilibrium point (x_o, y_o) for given values of the parameters (λ, p) , where $[f(x_o, y_o, \lambda, p) \ g(x_o, y_o, \lambda, p)]^T = 0$ ($\dot{x}=0$). Thus, by linearizing (1) at (x_o, y_o, λ, p) , it follows that

$$\begin{bmatrix} \Delta \dot{x} \\ 0 \end{bmatrix} = \underbrace{\begin{bmatrix} J_1 & J_2 \\ J_3 & J_4 \end{bmatrix}}_J \begin{bmatrix} \Delta x \\ \Delta y \end{bmatrix} \quad (2)$$

where J is the system Jacobian, and $J_1 = \partial f / \partial x|_0$, $J_2 = \partial f / \partial y|_0$, $J_3 = \partial g / \partial x|_0$, and $J_4 = \partial g / \partial y|_0$. If J_4 is non-singular, the system eigenvalues can be readily computed by eliminating the vector of algebraic variable Δy in (2), i.e.

$$\Delta \dot{x} = (J_1 - J_2 J_4^{-1} J_3) \Delta x = A \Delta x \quad (3)$$

In this case, the DAE system can then be reduced to a set of ODE equations [17]. Hence, bifurcations on power system models are typically detected by monitoring the eigenvalues of matrix A as the system parameters (λ, p) change.

B. Hopf Bifurcations

Hopf bifurcations are also known as oscillatory bifurcations. Such bifurcations are characterized by stable or unstable periodic orbits emerging around an equilibrium point, and can be studied with the help of linearized analyses, as these bifurcations are associated with a pair of purely imaginary eigenvalues of the state matrix A [16]. Thus, consider the dynamic power system (1), when the parameters λ and/or p vary, the equilibrium points (x_o, y_o) change, and so do the eigenvalues of the corresponding system state matrix A in (3). These equilibrium points are asymptotically stable if all the eigenvalues of the system state matrix have negative real parts. As the parameters change, the eigenvalues associated with the corresponding equilibrium point change as well. The point where a complex conjugate pair of eigenvalues reach the imaginary axis with respect to the changes in (λ, p) , say $(x_o, y_o, \lambda_o, p_o)$, is known as a Hopf bifurcation point; at this point, certain transversality conditions should be satisfied [16].

The transversality conditions basically state that a Hopf bifurcation corresponds to a system equilibrium point with a pair of purely imaginary eigenvalues with all other eigenvalues having non-zero real parts, and that the pair of bifurcating or critical eigenvalues cross the imaginary axis as the parameters (λ, p) change, yielding oscillations in the system.

Electromechanical oscillation problems have been classically associated with a pair of eigenvalues of system equilibria (operating points) jumping the imaginary axis of the complex plane, from the left half-plane to the right half-plane, when the system undergoes sudden changes, typically produced by system contingencies (e.g. line outages). If this particular oscillatory problem is studied using more gradual changes in the system,

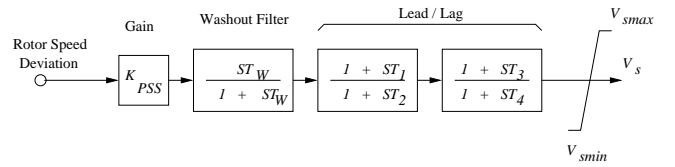


Fig. 1. PSS model used for simulations [6], where V_s is an additional input signal for the AVR.

such as changes on slow varying parameters like system loading, it can be directly viewed as a Hopf bifurcation problem, as suggested in [9]. Thus, in the current paper, Hopf bifurcation theory is used to analyze the appearance of electromechanical oscillations on a test system due to a line outage, and to devise damping techniques based on PSS, SVC and STATCOM controllers, as shown in Section IV.

C. Power System Stabilizers [6]

A PSS can be viewed as an additional block of a generator excitation control or AVR, added to improve the overall power system dynamic performance, especially for the control of electromechanical oscillations. Thus, the PSS uses auxiliary stabilizing signals such as shaft speed, terminal frequency and/or power to change the input signal to the AVR. This is a very effective method of enhancing small-signal stability performance on a power system network. The block diagram of the PSS used in the paper is depicted in Fig. 1.

In large power systems, participation factors corresponding to the speed deviation of generating units can be used for initial screening of generators on which to add PSS. However, a high participation factor is a necessary but not sufficient condition for a PSS at the given generator to effectively damp oscillation. Following the initial screening a more rigorous evaluation using residues and frequency response should be carried out to determine the most suitable locations for the stabilizers.

D. SVC

SVC is basically a shunt connected static var generator/load whose output is adjusted to exchange capacitive or inductive current so as to maintain or control specific power system variables; typically, the controlled variable is the SVC bus voltage. One of the major reasons for installing a SVC is to improve dynamic voltage control and thus increase system loadability. An additional stabilizing signal, and supplementary control, superimposed on the voltage control loop of a SVC can provide damping of system oscillation as discussed in [9], [10].

In this paper, the SVC is basically represented by a variable reactance with maximum inductive and capacitive limits to control the SVC bus voltage, with an additional control block and signals to damp oscillations, as shown in Fig. 2.

E. STATCOM

The STATCOM resembles in many respects a synchronous compensator, but without the inertia. The basic electronic block of a STATCOM is the Voltage Source Converter (VSC), which in general converts an input dc voltage into a three-phase output

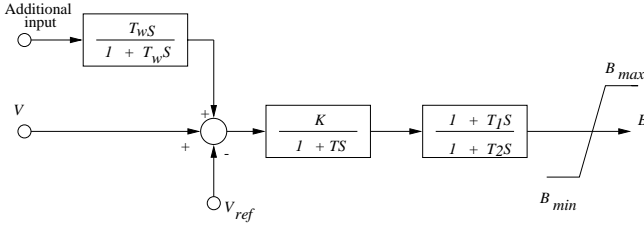


Fig. 2. Structure of SVC controller with oscillation damping, where B is the equivalent shunt susceptance of the controller.

voltage at fundamental frequency, with rapidly controllable amplitude and phase angle. In addition to this, the controller has a coupling transformer and a dc capacitor. The control system can be designed to maintain the magnitude of the bus voltage constant by controlling the magnitude and/or phase shift of the VSC output voltage.

The STATCOM is modelled here using the model described in [18], which is a fundamental frequency model of the controller that accurately represents the active and reactive power flows from and to the VSC. The model is basically a controllable voltage source behind an impedance with the representation of the charging and discharging dynamics, of the dc capacitor, as well as the STATCOM ac and dc losses. A phase control strategy is assumed for control of the STATCOM bus voltage, and additional control block and signals are added for oscillation damping, as shown in Fig. 3.

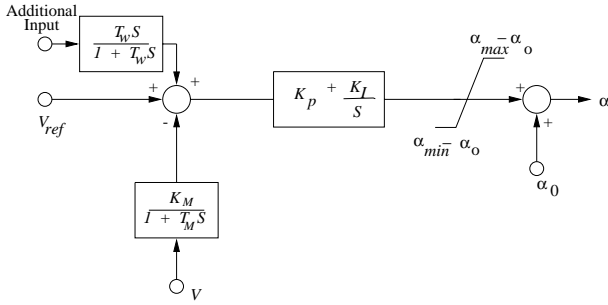


Fig. 3. STATCOM phase control with oscillation damping, where α is the phase shift between the controller VSC ac voltage and its bus voltage V .

III. OSCILLATION CONTROL USING FACTS

Even though it is a costly option when compared to the use of PSS for oscillation control, there are additional benefits of FACTS controllers. Besides oscillation control, FACTS local voltage control capabilities allow an increase in system loadability [19], which is not possible at all with PSS.

There are two major issues involved in FACTS controller design, apart from size and type. One is the placement, and the other is the choice of control input signal to achieve the desired objectives. For oscillation damping, the controller should be located to efficiently bring the critical eigenvalues into the open left half plane. This location might not correspond to the best placement to increase system loadability and improve voltage regulation, as shown in Section IV for the test system used. There are some methods suggested in the literature based on mode controllability and eigenvalue sensitivity analysis for

proper FACTS controller location (e.g. [14]). A new method based on extended eigen analysis is proposed here to determine the suitable location of a shunt FACTS controller for oscillation control. For the best choice of control signal, a mode observability index is used [14].

A. Shunt FACTS Controllers Placement

In calculating the eigenvalues of the system, the linearized DAE system equations can be used instead of the reduced system state matrix; this is popularly referred to as the generalized eigenvalue problem. Its major advantage is that sparse matrix techniques can be used to speed up the computation. Furthermore, the extended eigenvector can be used to identify the dominant algebraic variable associated with the critical mode. Thus the eigenvalue problem can be restated as

$$\begin{bmatrix} J_1 & J_2 \\ J_3 & J_4 \end{bmatrix} \begin{bmatrix} v_1 \\ v_2 \end{bmatrix} = \mu \begin{bmatrix} v_1 \\ 0 \end{bmatrix} \quad (4)$$

where μ is the eigenvalue and $[v_1 \ v_2]^T$ is the extended eigenvector of μ , with

$$v_2 = -J_4^{-1} J_3 v_1$$

Entries in v_2 correspond to the algebraic variables at each bus (e.g. voltages and angles, or real and imaginary voltages). In this case, real and imaginary voltages are used as the algebraic variables at each bus. A shunt FACTS controller, which directly controls voltage magnitudes, can be placed by identifying the maximum entry in v_2 associated with a load bus and the critical mode. Thus, assuming that

$$v_2 = \begin{bmatrix} v_{2V_{1r}} \\ v_{2V_{1i}} \\ \vdots \\ v_{2V_{nr}} \\ v_{2V_{ni}} \end{bmatrix}$$

where v_{2V} corresponds to the complex eigenvector associated with the real (r) and imaginary (i) components of the load bus voltages, i.e. $v_{2V_{kr}}$ and $v_{2V_{ki}}$ for load bus k , the magnitudes

$$v_{2V_k} = |v_{2V_{kr}} + jv_{2V_{ki}}|$$

are ranked in descending order. The largest entries of v_{2V_k} are then used to identify the candidate load buses for placement of shunt FACTS controllers. Clearly, this methodology is computationally more efficient than methods based on mode controllability indices.

B. Controls

The introduction of SVC and STATCOM controllers at an appropriate location, by itself does not provide adequate damping, as the primary task of the controllers is to control voltage. Hence, in order to increase the system damping, it is necessary to add an additional control block with an appropriate input signal.

The desired additional control input signal should be preferably local to avoid problems associated with remote signal control. Typical choices of local signals are real/reactive power flows and line currents in the adjacent lines. Here, a mode observability index was employed to determine the best input signal [14]. This additional signal is fed through a washout control block to avoid affecting steady state operation of the controller, and an additional lead-lag control block is used to improve dynamic system response, as shown in Figs. 2 and 3.

IV. RESULTS

All simulation results presented in this section are obtained for a slightly modified version of the IEEE 50 machine system, an approximated model of an actual power system that was developed as a benchmark for stability studies [20]. It consist of 145 buses and 453 lines, including 52 fixed-tap transformers. Seven of the generators are modeled in detail with IEEE ST1a exciters [22], whereas the rest of the generators are modeled only with their swing equations. The loads are modeled as constant impedances for all stability studies, and as PQ loads to obtain the PV curves. There are about 60 loads for a total load of 2.83 GW and 0.8 Gvar. The IEEE 50 machine system shows a wide range of dynamic characteristics, presenting low frequency oscillations at high loading levels.

A. Analytical Tools

P-V or nose curves of the system for various contingencies with and without controllers were obtained with the help of the UWPFLOW [21]. Modal analysis (eigenvalues analysis) and time domain simulations were carried out using the Power System Toolbox (PST) [22].

UWPFLOW is a research tool that has been designed to determine maximum loadability margins in power systems associated with saddle-node and limit induced bifurcations. The program has detailed static models of various power system elements such as generators, loads, HVDC links, and various FACTS controllers, particularly SVC and STATCOM controllers under phase and PWM control, representing control limits with accuracy for all models.

PST is a MATLAB-based analysis toolbox developed to perform stability studies in power systems. It has several tools with graphical features, of which the transient stability and small signal stability tools were used to obtain the results presented here.

B. Simulation Results

Figure 4 shows the P-V curves, including the operating point at which a Hopf bifurcation is observed (HB point), for two different contingencies in the system (lines 79-90 and 90-92, as these are two of the most heavily loaded line in the weakest area of the system). These curves were obtained for a specific load and generation direction by increasing the active and reactive powers in the loads as follows:

$$P = P_o(1 + \lambda)$$

$$Q = Q_o(1 + \lambda)$$

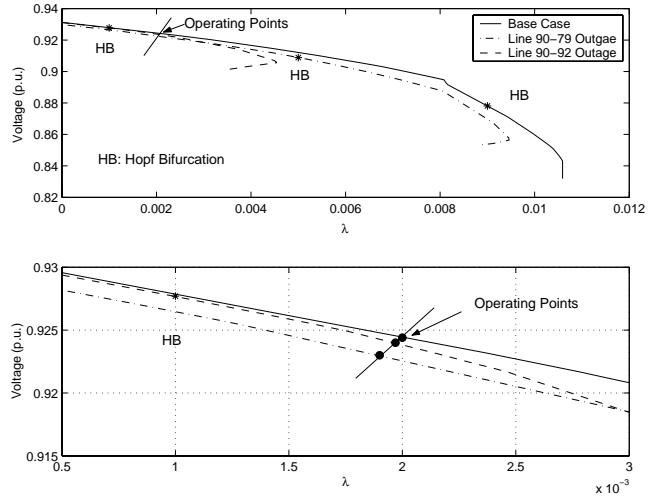


Fig. 4. (a) P-V curves at bus 92 for different contingencies, and (b) enlarged P-V curves around the operating point.

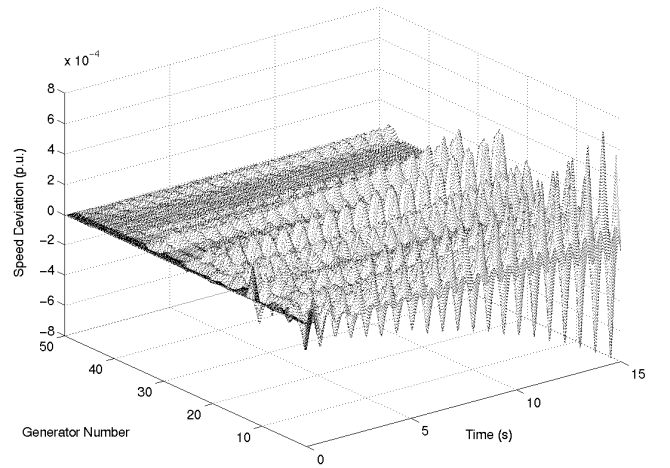


Fig. 5. Oscillations due to a Hopf bifurcation triggered by line 90-92 outage ($\lambda=0.002$ p.u.).

where P_o and Q_o correspond to the base loading conditions and λ is loading factor. The “current” operating conditions are assumed to correspond to a value $\lambda = 0.002$ p.u. The operating condition “line” depicted on Fig. 4 defines the steady state points for the base system topology and two contingencies under consideration, assuming that the load is being modeled as a constant impedance in small and large disturbance stability studies; this is the reason why this line is not vertical.

As one can see from the P-V curves, a Hopf bifurcation problem is triggered by the line 90-92 outage, since the load line yields an equilibrium point beyond the HB point on the corresponding PV curve. In order to study the effect of this bifurcation in the system, a time domain simulation was performed for the corresponding contingency at the given operating conditions. As can be seen in Fig. 5, the Hopf bifurcation leads the system to an oscillatory unstable condition.

The dominant state variables related to the Hopf bifurcation mode, which are responsible for the oscillation, were identified through a participation factor analysis, as previously explained. The state variables of the machines associated with the Hopf

TABLE I
PARTICIPATION FACTOR ANALYSIS

Base Case			Line 90-92 outage		
State	Bus	P. Factor	State	Bus	P. Factor
ω	93	1.0000	δ	104	1.0000
δ	93	1.0000	ω	104	1.0000
E'_q	93	0.3452	E'_q	104	0.1715
ω	124	0.1734	δ	111	0.2622
δ	124	0.1728	ω	111	0.2622
Ψ''_q	93	0.1720	δ	121	0.1713
ω	121	0.1206	ω	121	0.1709

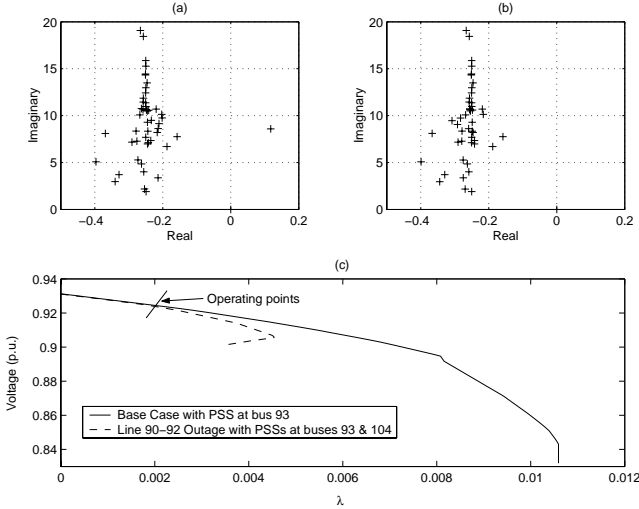


Fig. 6. Line 90-92 outage: (a) Some eigenvalues with PSS at bus 93; (b) eigenvalues with PSS's at bus 93 and 104; (c) P-V curves.

bifurcations for the base and the line 90-92 outage, and the corresponding participation factors are given in Table I. It is interesting to see that with the line 90-92 outage the critical mode differs from that in the base. Thus, the PSS at bus 93, which stabilizes the base case, is unable to stabilize the contingency case; for the latter, a PSS at bus 104 is required for stability. Time domain analysis confirms the linear analysis, as can be seen from Figs. 6 and 7.

SVC and STATCOM controllers were considered as the other possible choices to control system oscillations. To find out the suitable location for the shunt FACTS controllers, the proposed extended eigen analysis technique was applied to the test system. Thus, the algebraic eigenvector v_2 was computed for the Hopf bifurcation point at the base case, resulting in seven load buses as possible candidates for placement of a SVC/STATCOM. Table II shows the bus and associated value of $|v_{2v_k}|$; the last two columns correspond to the critical eigenvalue when a SVC or a STATCOM are placed on the corresponding buses. These results were obtained for "typical" ± 150 MVar SVC and STATCOM controllers without the additional control loop for damping oscillations, and indicate that bus 125 is the best candidate location to prevent the Hopf bifurcation problem in the base case; this was confirmed by time domain simulations.

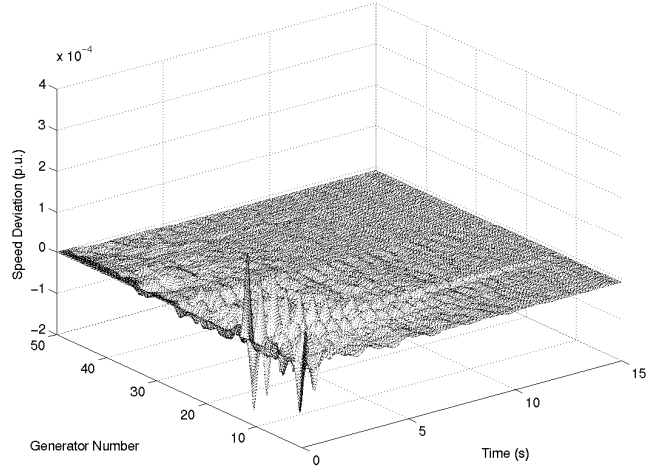


Fig. 7. Oscillation damping with PSS at bus 93 and 104 for line 90-92 outage ($\lambda=0.002$ p.u.).

TABLE II
CRITICAL EIGENVALUES WITH SVC AND STATCOM AT DIFFERENT LOCATIONS

Bus	$ v_{2v_k} \times 10^{-2}$	Critical eigenvalue	
		SVC	STATCOM
125	1.5980	$-0.014 \pm j6.536$	$-0.022 \pm j6.527$
133	1.3450	$-0.006 \pm j6.493$	$-0.018 \pm j6.504$
68	1.0786	$-0.005 \pm j6.480$	$-0.015 \pm j6.501$
123	1.0618	$0.005 \pm j6.481$	$-0.004 \pm j6.491$
75	1.0068	$0.029 \pm j6.433$	$0.020 \pm j6.448$
29	0.9803	$0.016 \pm j6.459$	$0.013 \pm j6.464$
28	0.9736	$0.016 \pm j6.458$	$0.013 \pm j6.464$

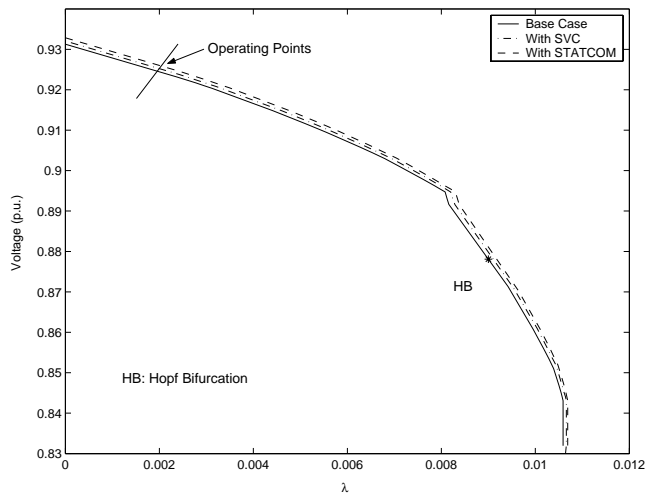


Fig. 8. P-V curves with SVC and STATCOM controllers for the base case.

TABLE III
LOADING MARGIN WITH DIFFERENT CONTROLLERS

Controllers	Maximum Loading Margin (p.u.)	
	Base Case	Line 90-92 outage
no controller	0.01059	0.00454
PSS	0.01059	0.00454
SVC at 125	0.01066	0.01059
STATCOM at 125	0.01069	0.01066
SVC at 107	0.01069	0.01061
STATCOM at 107	0.01078	0.01071

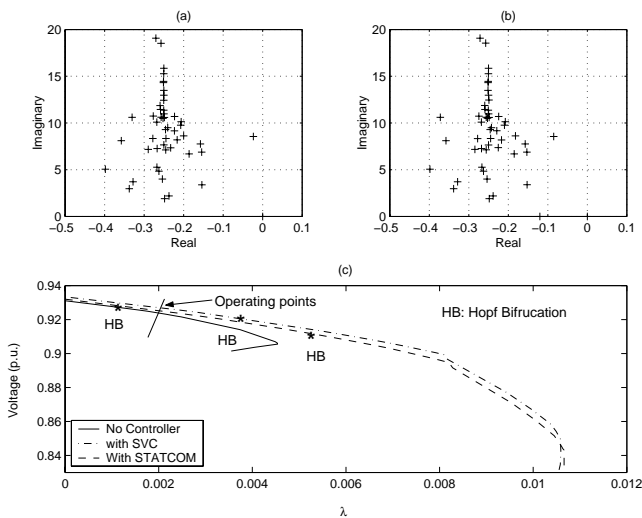


Fig. 9. Line 90-92 outage: (a) Some eigenvalues with SVC; (b) eigenvalues with STATCOM; (c) P-V curves with SVC and STATCOM.

Figure 8 shows the P-V curves for SVC and STATCOM controllers located at bus 125, showing that the Hopf bifurcation can be removed for the base case. Observe that the loadability margin for the system does not increase significantly; this is due to the fact that voltage stability analysis yields bus 107 as the best location to maximize system loadability, and that the size of the SVC/STATCOM chosen is not very significant for these purposes. Table III shows the maximum loadability margins for different system conditions and controllers under study. Notice that the SVC and STATCOM controllers significantly increase system loadability when the contingency is applied.

Figure 9 shows the eigenvalue plot with SVC and STATCOM controllers at bus 125, and the corresponding P-V curves for the line 90-92 outage case. It is interesting to see that the SVC and STATCOM work well for the given contingency, even though the optimal placement in this case should be bus 77 based on the extended eigen analysis. The P-V curves show that both the static loading margin and the dynamic stability margin (margin between the current operating point and the Hopf bifurcation point) increase when SVC and STATCOM controllers are introduced.

Observe that the damping introduced by the SVC and STATCOM controllers with only voltage control was lower than that provided by the PSS's. Hence, additional control signals were considered to enhance damping, using mode observability in-

TABLE IV
ADDITIONAL CONTROL INPUT SIGNALS

Line	Signal	OI	Line	Signal	OI
67-125	I	1.0955	121-125	I	0.3269
	P	1.1099		P	0.3319
	Q	0.5473		Q	0.0165
125-132	I	0.6656	122-125	I	0.1090
	P	0.6809		P	0.1123
	Q	0.1075		Q	0.0165

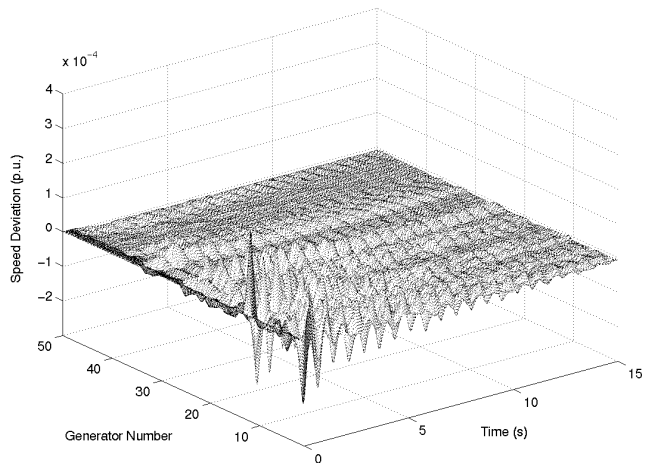


Fig. 10. Oscillation damping with SVC and additional control loop for line 90-92 outage ($\lambda = 0.002$ p.u.).

trices (OI) to identify the best additional signal. Table IV shows the mode OI obtained for different control input signals from the adjacent lines to the controller location with open loop control. According to this table, real power flow in line 67-125 is the best choice; this was confirmed by time domain simulations. Figures 10 and 11 show the time domain simulations obtained for the line 90-92 outage at the given operating point with SVC and STATCOM controllers and additional control loops, respectively. The best oscillation damping is obtained with the PSS controller, as expected, due to the direct control of the state variables and generator that yield the problem. Furthermore, the STATCOM provides better damping than the SVC, which is to be expected, as this controller is able to transiently exchange active power with the system.

It is important to mention that in the current test system only certain oscillation modes and contingencies were considered for placing the PSS's, resulting in only two of these controllers being introduced in the system. In practice, PSS's should be considered for all generators with fast static exciters, which for the given system would correspond to 7 generators.

V. CONCLUSIONS

This paper presents the direct correlation between typical electromechanical oscillations in power systems and Hopf bifurcations, so that Hopf bifurcation theory can be used to design remedial measures to resolve oscillation problems. A placement technique is proposed to identify and rank suitable locations for placing shunt FACTS controllers, for the purpose of

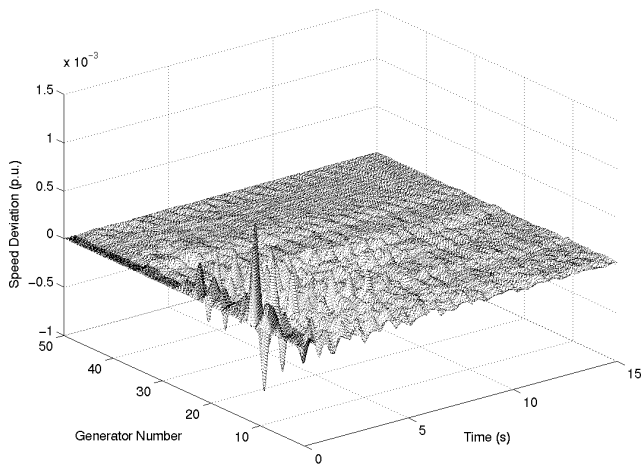


Fig. 11. Oscillation damping with STATCOM and additional control loop for line 90-92 outage ($\lambda = 0.002$ p.u.).

oscillation control.

The paper demonstrates that inter-area oscillations, which are typically damped using PSS controllers on generators, can be adequately handled by properly placing SVC or STATCOM controllers with additional controls on the transmission side.

Series connected FACTS controllers have been applied for oscillation control in power systems. This paper demonstrates that shunt-connected FACTS controllers, when properly placed and controlled, can also effectively damp system oscillations. This makes these types of controllers very appealing when compared to series-connected controllers, given their additional bus voltage control characteristics and lower overall costs.

Even though it has been shown that SVC and STATCOM controllers significantly increase stability margins, especially when contingencies occur, and that voltage profiles improve throughout the system, an overall cost-benefit analysis must be carried out when considering the use of these FACTS controllers for damping oscillations, given their relatively high costs when compared to PSS's.

REFERENCES

- [1] Y.-Y. Hsu, S.-W. Shyue, and C.-C. Su, "Low Frequency Oscillation in Longitudinal Power Systems: Experience with Dynamic Stability of Taiwan's Power System," *IEEE Trans. Power Systems*, Vol. 2, No. 1, pp. 92–100, Feb. 1987.
- [2] D. N. Koterev, C. W. Taylor, and W. A. Mittelstadt, "Model Validation for the August 10, 1996 WSCC System Outage," *IEEE Trans. Power Systems*, Vol. 14, No. 3, pp. 967–979, Aug. 1999.
- [3] G. Rogers, *Power System Oscillations*, Kluwer, Norwell, MA, 2000.
- [4] M. Klein, G. J. Rogers, and P. Kundur, "A Fundamental Study of Inter-Area Oscillation in Power Systems," *IEEE Trans. Power Systems*, Vol. 6, No. 3, pp. 914–921, Aug. 1991.
- [5] N. Mithulananthan and S. C. Srivastava, "Investigation of a Voltage Collapse Incident in Sri Lanka's Power System Network," *Proc. of EMPD'98, Singapore*, IEEE Catalogue No. 98EX137, pp. 47–52, Mar. 1998.
- [6] P. Kundur, *Power System Stability and Control*, McGraw Hill, New York, 1994.
- [7] E. H. Abed and P. P. Varaiya, "Nonlinear Oscillation in Power Systems," *Int. J. Electric Power and Energy Systems*, Vol. 6, pp. 37–43, 1984.
- [8] C. A. Cañizares and S. Hranilovic, "Transcritical and Hopf Bifurcations in AC/DC Systems," *Proc. Bulk Power System Voltage Phenomena III—Voltage Stability and Security*, Davos, Switzerland, pp. 105–114, Aug. 1994.

- [9] M. J. Launberg, M. A. Pai, and K. R. Padiyar, "Hopf Bifurcation Control in Power System with Static Var Compensators," *Int. J. Electric Power and Energy Systems*, Vol. 19, No. 5, pp. 339–347, 1997.
- [10] N. Mithulananthan, C. A. Cañizares, and John Reeve, "Hopf Bifurcation Control in Power System Using Power System Stabilizers and Static Var Compensators," *Proc. of NAPS'99*, pp. 155–163, San Luis Obispo, California, Oct. 1999.
- [11] C. A. Cañizares, Editor, "Voltage Stability Assessment, Procedures and Guides," IEEE/PES Power Systems Stability Subcommittee, Draft, July 1999. Available at <http://www.power.uwaterloo.ca>.
- [12] N. G. Hingorani, "Flexible AC Transmission Systems," *IEEE Spectrum*, pp. 40–45, Apr. 1993.
- [13] H. F. Wang and F. J. Swift, "A Unified Model for the Analysis of FACTS Devices in Damping Power System Oscillations Part I: Single-machine Infinite-bus Power Systems," *IEEE Trans. Power Delivery*, Vol. 12, No. 2, pp. 941–946, Apr. 1997.
- [14] N. Yang, Q. Liu, and J. D. McCalley, "TCSC Controller Design for Damping Interarea Oscillations," *IEEE Trans. Power Systems*, Vol. 13, No. 4, pp. 1304–1310, Nov. 1998.
- [15] E. Uzunovic, C. A. Cañizares, and John Reeve, "EMTP Studies of UPFC Power Oscillation Damping," *Proc. of NAPS'99*, pp. 155–163, San Luis Obispo, California, Oct. 1999.
- [16] R. Seydel, *Practical Bifurcation and Stability Analysis: From Equilibrium to Chaos*, Second Edition, Springer-Verlag, New York, 1994.
- [17] D. J. Hill and I. M. Y. Mareels, "Stability Theory for Differential/Algebraic Systems with Application to Power Systems," *IEEE Trans. Circuits and Systems*, Vol. 37, No. 11, pp. 1416–1423, Nov. 1990.
- [18] C. A. Cañizares, "Power Flow and Transient Stability Models of FACTS Controllers for Voltage and Angle Stability Studies," *Proc. of the 2000 IEEE/PES Winter Meeting*, Singapore, 8 pages, Jan. 2000.
- [19] C. A. Cañizares and Z. T. Faur, "Analysis of SVC and TCSC Controllers in Voltage Collapse," *IEEE Trans. on Power Systems*, Vol. 14, No. 1, pp. 158–165, Feb. 1999.
- [20] V. Vittal, Chairman, "Transient Stability Test Systems for Direct Stability Methods," IEEE committee report, *IEEE Trans. on Power Systems*, Vol. 7, No. 1, pp. 37–42, Feb. 1992.
- [21] C. A. Cañizares, et al., "PFLOW: Continuation and Direct Methods to Locate Fold Bifurcations in AC/DC/FACTS Power Systems," University of Waterloo, August 1998. Available at <http://www.power.uwaterloo.ca>.
- [22] "Power System Toolbox Ver. 2.0: Dynamic Tutorial and Functions," Cherry Tree Scientific Software, Colborne, Ontario, 1999.

PLACE
PHOTO
HERE

Nadarajah Mithulananthan was born in Sri Lanka. He received his B.Sc. (Eng.) and M.Eng. degrees from the University of Peradeniya, Sri Lanka, and the Asian Institute of Technology, Thailand, in May 1993 and August 1997, respectively. Mr. Mithulananthan has worked as an Electrical Engineer at the Generation Planning Branch of the Ceylon Electricity Board, and as a Researcher at Chulalongkorn University, Thailand. He is currently a Ph.D. candidate at the University of Waterloo working on applications and control design of FACTS controllers.

PLACE
PHOTO
HERE

Claudio A. Cañizares received in April 1984 the Electrical Engineer diploma from the Escuela Politécnica Nacional (EPN), Quito-Ecuador, where he held different teaching and administrative positions from 1983 to 1993. His M.Sc. (1988) and Ph.D. (1991) degrees in Electrical Engineering are from the University of Wisconsin-Madison. Dr. Cañizares is currently an Associate Professor and the Associate Chair for Graduate Studies at the E&CE Department of the University of Waterloo, and his research activities mostly concentrate in studying stability, modeling and computational issues in ac/dc/FACTS systems.

PLACE
PHOTO
HERE

John Reeve received the B.Sc., M.Sc., Ph.D. and D.Sc. degrees from the University of Manchester (UMIST). After employment in the development of protective relays for English Electric, Stafford, between 1958 and 1961, he was a lecturer at UMIST until joining the University of Waterloo in 1967, where he is currently an Adjunct Professor in the Department of Electrical & Computer Engineering. He was a project manager at EPRI, 1980-81, and was with IREQ, 1989-1990. His research interests since 1961 have been HVDC transmission and high power electronics. He is the President of John Reeve Consultants Limited.

Dr. Reeve was chair of the IEEE DC Transmission Subcommittee for 8 years, and is a member of several IEEE and CIGRE Committees on dc transmission and FACTS. He was awarded the IEEE Uno Lamm High Voltage Direct Current Award in 1996.

PLACE
PHOTO
HERE

Graham Rogers graduated in Electrical Engineering, with first class honors, from Southampton University in 1961. From 1961 to 1964 he was a consultant Mathematician with A.E.I. (Rugby) Ltd. From 1964 until 1978 he was Lecturer in Electrical Engineering at Southampton University. He immigrated to Canada in 1978 to work for Ontario Hydro in the Power System Planning Division. Since his retirement in 1993 he has operated Cherry Tree Scientific Software. He was Associate Professor (part time) at McMaster University from 1982 to 1996 and Visiting

Professor at I.I.T. Madrid in 1997. He is currently Adjunct Associate Professor at the University of Toronto. He is a member of several IEEE Power Engineering Society Working Groups and was an Associate Editor of IEEE Transactions on Control System Technology from 1994 to 1997.